

OPEN

Elevated CO₂ regulates the Wnt signaling pathway in mammals, *Drosophila melanogaster* and *Caenorhabditis elegans*

Masahiko Shigemura¹, Emilia Lecuona¹, Martín Angulo², Laura A. Dada¹, Melanie B. Edwards¹, Lynn C. Welch¹, S. Marina Casalino-Matsuda¹, Peter H. S. Sporn^{1,3}, István Vadász⁴, Iiro Taneli Helenius^{1,11}, Gustavo A. Nader⁵, Yosef Gruenbaum⁶, Kfir Sharabi^{7,8}, Eoin Cummins⁹, Cormac Taylor⁹, Ankit Bharat¹⁰, Cara J. Gottardi¹, Greg J. Beitel¹¹, Naftali Kaminski¹², G. R. Scott Budinger¹, Sergejs Berdnikovs¹³ & Jacob I. Sznajder^{1*}

Carbon dioxide (CO₂) is sensed by cells and can trigger signals to modify gene expression in different tissues leading to changes in organismal functions. Despite accumulating evidence that several pathways in various organisms are responsive to CO₂ elevation (hypercapnia), it has yet to be elucidated how hypercapnia activates genes and signaling pathways, or whether they interact, are integrated, or are conserved across species. Here, we performed a large-scale transcriptomic study to explore the interaction/integration/conservation of hypercapnia-induced genomic responses in mammals (mice and humans) as well as invertebrates (*Caenorhabditis elegans* and *Drosophila melanogaster*). We found that hypercapnia activated genes that regulate Wnt signaling in mouse lungs and skeletal muscles *in vivo* and in several cell lines of different tissue origin. Hypercapnia-responsive Wnt pathway homologues were similarly observed in secondary analysis of available transcriptomic datasets of hypercapnia in a human bronchial cell line, *flies* and *nematodes*. Our data suggest the evolutionarily conserved role of high CO₂ in regulating Wnt pathway genes.

Cells and tissues sense and respond to changes in concentration of gaseous molecules through evolutionarily conserved pathways. Oxygen- and nitric oxide-activated cellular signaling pathways are well described^{1,2}, but much less is known about the mechanisms by which non-excitatory cells sense and respond to changes in carbon dioxide (CO₂) concentrations^{3,4}. In humans, an increase in CO₂ levels (hypercapnia) is a consequence of inadequate alveolar gas exchange in patients with lung diseases such as the acute respiratory distress syndrome^{5,6}, chronic obstructive pulmonary disease⁷ and others^{4,8}. Although initially thought to be benign or even protective^{5,6}, it is

¹Division of Pulmonary and Critical Care, Department of Medicine, Feinberg School of Medicine, Northwestern University, Chicago, IL, United States of America. ²Pathophysiology Department, School of Medicine, Universidad de la República, Montevideo, Uruguay. ³Medical Service, Jesse Brown Veterans Affairs Medical Center, Chicago, IL, United States of America. ⁴Department of Internal Medicine, Justus Liebig University, Universities of Giessen and Marburg Lung Center, German Center for Lung Research, and The Cardio-Pulmonary Institute, Giessen, Germany. ⁵Department of Kinesiology and Huck Institutes of the Life Sciences, The Pennsylvania State University, State College, PA, United States of America. ⁶Department of Genetics, Institute of Life Sciences, Hebrew University of Jerusalem, Givat Ram, Jerusalem, Israel. ⁷Department of Cancer Biology, Dana-Farber Cancer Institute, Boston, MA, United States of America. ⁸Department of Cell Biology, Harvard Medical School, Boston, MA, United States of America. ⁹School of Medicine, Systems Biology Ireland and the Conway Institute of Biomolecular and Biomedical Research, University College Dublin, Belfield, Dublin, 4, Ireland. ¹⁰Division of Thoracic Surgery, Department of Medicine, Feinberg School of Medicine, Northwestern University, Chicago, IL, USA. ¹¹Department of Molecular Biosciences, Northwestern University, Evanston, IL, United States of America. ¹²Department of Internal Medicine, Section of Pulmonary, Critical Care, and Sleep Medicine, Yale School of Medicine, New Haven, CT, United States of America. ¹³Division of Allergy and Immunology, Feinberg School of Medicine, Northwestern University Feinberg School of Medicine, Chicago, IL, United States of America. *email: j-sznajder@northwestern.edu

becoming increasingly evident that hypercapnia has significant pathophysiological effects that may be deleterious to organs such as the lung^{7–10} and skeletal muscles¹¹. Recent discoveries suggest that elevation of CO₂ activates specific signal transduction pathways with adverse consequences for cellular and organismal functions not only in mammals^{7,9,12–14}, but also fish¹⁵, fly *Drosophila melanogaster*^{16,17}, and nematode *Caenorhabditis elegans*^{17,18}. Hypercapnia has also been reported to alter gene expression in different tissues, cells and species^{7,12,16,18,19}. However, a systems-level understanding of elevated CO₂ effects and of how they are integrated into signaling pathway network, and whether hypercapnia-induced gene programs are similar in different tissues/cells and species is not completely understood.

Here, we performed a large-scale comparative transcriptomic study to explore the interaction/integration/conservation of hypercapnia-responsive genes combining multi-tissue microarray analysis in mice with secondary analysis of transcriptomic datasets of hypercapnia in human bronchial epithelial cells (HBEC)¹², *Drosophila melanogaster*¹⁶ and *Caenorhabditis elegans*¹⁸. We found that hypercapnia activates genes that regulate Wnt signaling in mouse cells, lungs and skeletal muscles. Hypercapnia-activated Wnt pathway homologues were similarly observed in the human bronchial cells, *flies* and *nematodes* at gene expression level. Our data suggest that the role of high CO₂ as a gaso-signal in regulating Wnt signaling pathways is evolutionarily conserved.

Results

Multi-tissue microarray analysis identifies functional similarity in gene networks across different mouse tissues exposed to normoxic hypercapnia.

In mammals, lung diseases are associated with suboptimal function of other metabolic organs including skeletal muscle²⁰. To elucidate whether hypercapnia activates conserved genes or gene networks governing specific signaling pathways on an organismal level, we performed a multi-tissue microarray analysis, contrasting available transcriptomic datasets in mouse lungs⁷ with microarray analysis of skeletal muscles, diaphragm and soleus, isolated from mice exposed to normoxic hypercapnia (60 to 80 mmHg = 10% CO₂ and 21% O₂) or sea-level room air for up to 7 days (Fig. 1). The microarray analysis in the lungs, as compared to the skeletal muscles, revealed increased number of differentially expressed genes (DEG) dependent on CO₂ exposure time (Fig. 1a), suggesting that the transcriptional response differs in terms of genes regulated and/or the kinetics of gene activation among the different tissues. Although up-regulated hypercapnia-responsive gene sets differed among the tissues, we found three genes of which was robustly represented in all the tissues, *Fzd9*, *Gm7120* and *LOC100044171*, at 7-day exposure conditions (Fig. 1a and Table S1). We next examined effects of hypercapnia on the functional categorization of the DEG in the tissues. A biological process analysis of the DEG was performed by the Protein ANalysis THrough Evolutionary Relationships (PANTHER) classification system (Fig. 1b). A network diagram constructed from the DEG at 7-day exposure conditions revealed groups of genes and pathways that shared common components (green circles) but was also comprised of lung-specific, diaphragm-specific, soleus-specific response to hypercapnic exposure (Fig. 1c, blue, yellow and red circles, respectively). Despite differences of gene signatures in biological processes observed among the tissues, an unbiased functional analysis of hypercapnia-responsive genes showed that the impact of hypercapnia on gene expression was highly similar. We found three functionally conserved gene networks in response to hypercapnia; Wnt signaling pathway, calcium ion (Ca²⁺) transport/signaling pathway and potassium ion (K⁺) transport (Fig. 1c). To identify transcription factors potentially regulatory for the hypercapnia-responsive genes and conserved in different tissues, we further analyzed our microarray data using an inference transcription factor analysis (Fig. S1). We identified several transcription factors regulatory for hypercapnia-responsive genes, as inferred from differential gene expression signatures of day-3, day-7, or both, hypercapnia responses.

Analysis of transcriptomic datasets of hypercapnia in a human bronchial cell line and invertebrates.

We next compared mouse hypercapnia gene signatures against transcriptomic datasets of normoxic hypercapnia in HBEC¹², *Caenorhabditis elegans*¹⁸ and *Drosophila melanogaster*¹⁶. We need to mention that high CO₂ exposure conditions in each dataset were somewhat different; 20% CO₂ exposure for 24 hours in HBEC, 19% CO₂ for 72 hours in *Caenorhabditis elegans* and 13% CO₂ for 24 hours in *Drosophila melanogaster*. The PANTHER classification system categorized DEG into signaling pathways in each dataset. Despite different conditions of high CO₂ exposure in each dataset, we found the DEG involved in Wnt signaling pathway overrepresented in the human bronchial cell line and invertebrates (Fig. 1d). Multiple gene components of the Wnt pathway were also detected in the DEG of mice, HBEC and invertebrates during hypercapnia (Fig. S2 and Table S2). These data suggest that the genes involved in the Wnt pathway are the highest prevalence group of hypercapnia-responsive genes that may be conserved across the tissues and organisms.

Validation of conserved Wnt pathway genes in the large-scale microarray analysis.

To validate our large-scale microarray data, quantitative real-time PCR (qRT-PCR) was performed using RNA isolated from different mouse tissues (lung and diaphragm skeletal muscle) and cells exposed to high CO₂ conditions (Fig. 2). For *in vivo* experiments, we examined expressions of *Fzd9*, *Wnt4*, *Wnt7a* and *Wnt8b* for the gene network of “Wnt signaling pathway” (Fig. 2a,b). The relative expression levels of *Fzd9* and *Wnt7a* exhibited the same regulatory trends as compared with the microarray analysis, suggesting that hypercapnia activates genes that regulate the Wnt signaling in mice tissues. We next examined expressions of genes validated in the tissues, *Fzd9* and *Wnt7a*, in a panel of mouse cell types; mouse lung epithelial (MLE)-12 cells representing as an epithelial lineage, airway smooth muscle (ASM) cells as the smooth muscle cell lineage and C2C12 myoblasts and myotubes as skeletal muscle lineage exposed to high (~120 mmHg = 20%) CO₂ and normoxia with an extracellular pH of 7.4. These cell lineages are one of the major cell components of the lung or skeletal muscle tissues and have been reported to show signal transduction pathways and the related-biological effects of hypercapnia as previously reported^{7,9,11}. *Fzd9* and *Wnt7a* expressions were tightly regulated and peaked at six hours after high CO₂ exposure in the lung cells, and at one hour in the skeletal muscle cells but not in the myotubes (Fig. 2c,d). We also

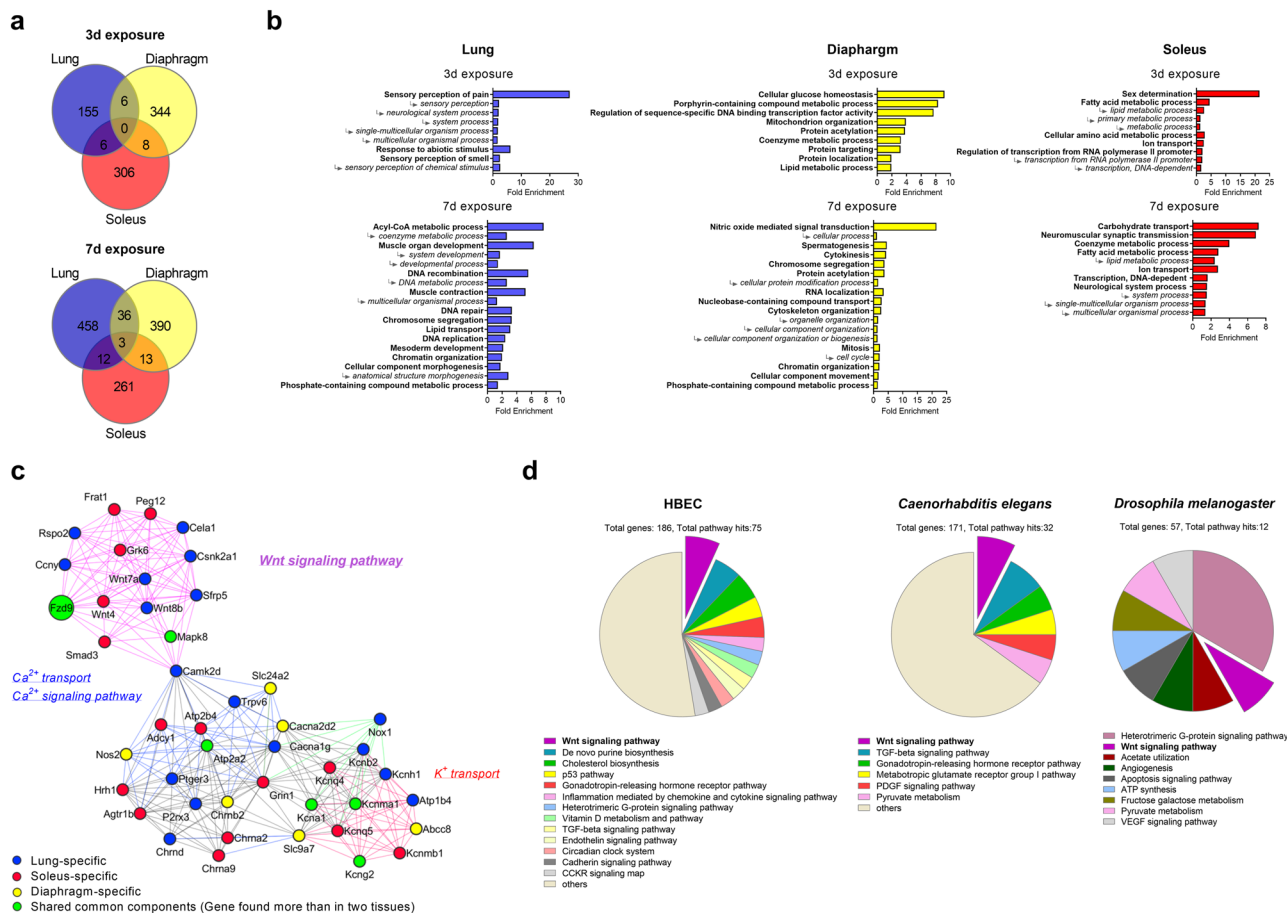


Figure 1. A large-scale transcriptomic study of hypercapnia to combine mouse multi-tissue microarray analysis with secondary analysis of available transcriptomic datasets. **(a–c)** C57BL/6 J mice were exposed to normoxic hypercapnia for 3 ($n = 4$) or 7 ($n = 3$) days or maintained in sea-level room air ($n = 3$). **(a)** Venn diagrams showing the overlap between DEG from lung, diaphragm and soleus. **(b)** Gene ontology analysis of the DEG in each tissue using the PANTHER GO-Slim Biological Process annotation dataset. Arrows indicate hierarchical grouping between GO terms. **(c)** A network diagram constructed from the DEG in each dataset at 7-day exposure conditions. The network diagram revealed groups of genes and pathways that shared common components (green circles) but was also comprised of lung-specific, diaphragm-specific, soleus-specific responsive to hypercapnic exposure (blue, yellow and red circles, respectively). **(d)** Secondary analysis of transcriptomic datasets of hypercapnia in HBEC, *Caenorhabditis elegans* and *Drosophila melanogaster*. PANTHER classification system categorized the DEG in each dataset into signaling pathways.

examined expression of *FZD9* and *WNT7a* in an immortalized human bronchial epithelial cell line BEAS-2B (Fig. 3a) and major Frizzled and Wnt ligand genes (*fz* and *wg*) in *Drosophila* S2 cells (macrophage like lineage) (Fig. 3b). Consistent with the data in mouse cells, hypercapnia caused transient increases in particular in Frizzled and WNT ligand gene expressions in the human and *fly* cells. Taken together, our data suggest that normoxic hypercapnia activates genes that regulate the Wnt signaling pathway across different cells, tissues and species.

Discussion

Elevation of CO₂ has been proposed to affect organismal pathobiology. In recent years, there is accumulating evidence on significant deleterious effects of elevated CO₂ *per se* on cell, tissue and organismal functions^{7,9,11–18,21,22}. However, little is known about the variation in the global transcriptional response to CO₂ elevation among different cell types, tissues or species. Here, we provide a new systems-level understanding of high CO₂-conserved effects across *nematodes*, *flies*, mice and humans regulating Wnt signaling pathway genes, which appears to be central to high CO₂ gaso-signal.

Our data suggest that hypercapnia leads to changes in the expression of genes involved in a variety of biological processes in mouse tissues. Interestingly, the gene network diagram constructed from the hypercapnia-responsive genes among the tissues revealed a functionally similar group of genes that activate Wnt signaling pathway, which was not previously known to be regulated by high CO₂. The Wnt pathway is a highly conserved signal transduction cascade in animals that has a critical role in many biological processes^{23–26}. Wnt signals are also known to activate more than one type of signaling cascade or cross-talk with other signaling pathways, and result in integrated, context-dependent cellular responses²³. We also observed hypercapnia-responsive Wnt pathway genes that were categorized into other signaling pathways (Table S2). The Wnt signaling pathway may cross-talk

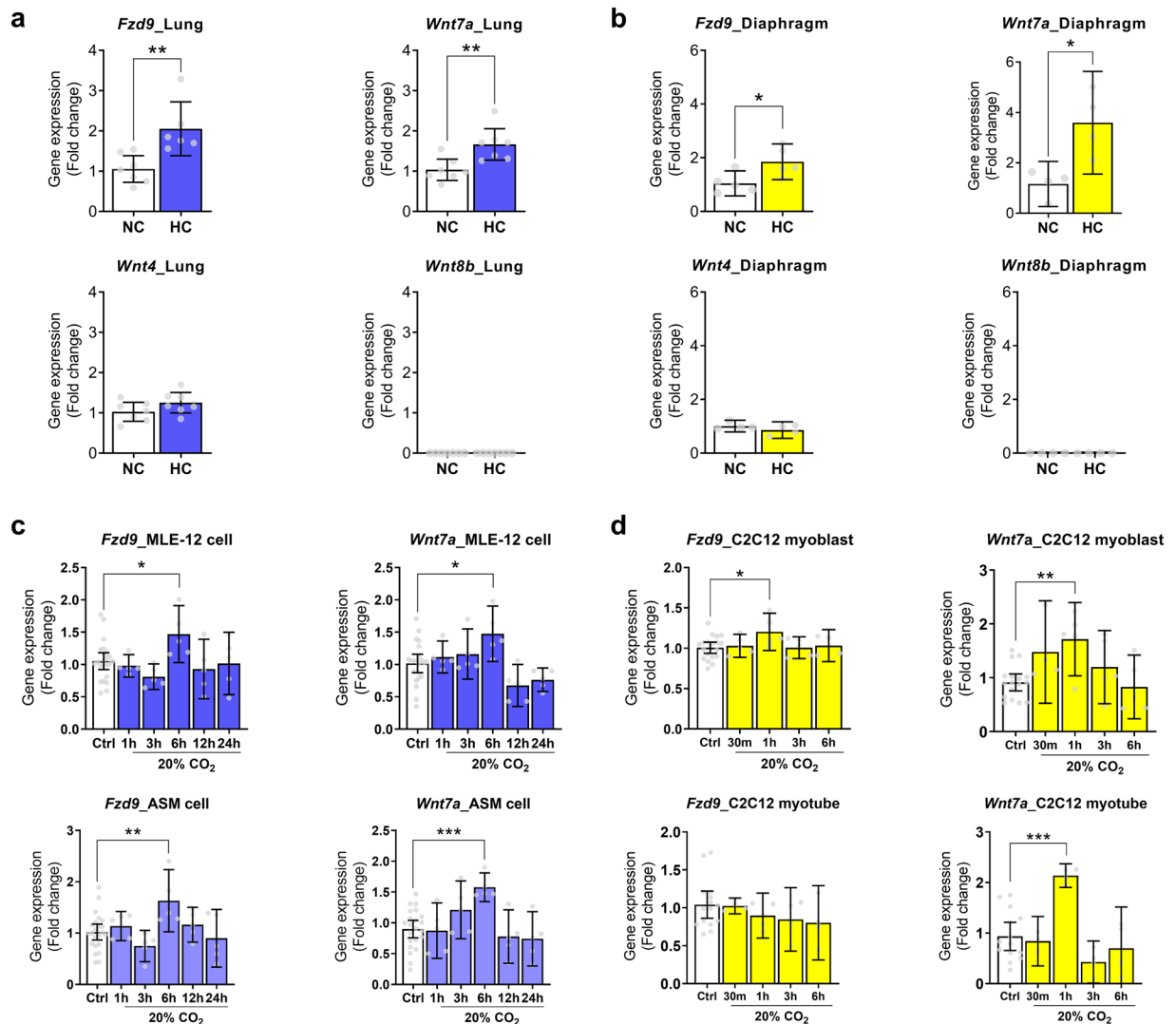


Figure 2. Validation of mouse multi-tissue microarray analysis. **(a,b)** Validation in mouse tissues. *Fzd9*, *Wnt4*, *Wnt7a*, and *Wnt8b* expression in the lung ($n = 6-7$) **(a)** and diaphragm skeletal muscle ($n = 4-5$) **(b)** from mice exposed to normoxic hypercapnia for 7 days. NC, normocapnia; HC, hypercapnia. **(c,d)** Validation in mouse lung and skeletal muscle cells. *Fzd9* and *Wnt7a* expressions in MLE-12 cells (Ctrl, $n = 22-23$; 20%CO₂, $n = 5$ per group), ASM cells (Ctrl, $n = 22-23$; 20%CO₂, $n = 5$ per group) **(c)**, or C2C12 myoblast (Ctrl, $n = 18-19$; 20%CO₂, $n = 4-5$ per group) or myotube (Ctrl, $n = 14-15$; 20%CO₂, $n = 3-4$ per group) **(d)** exposed to high CO₂ for up to 24 hours **(c)** or 6 hours **(d)**. Ctrl, control conditions. All values are represented as mean with error bars shown as the 95% confidence interval. * $p < 0.05$, ** $p < 0.01$, *** $p < 0.001$, unpaired two-tailed Student's *t* test or one-way ANOVA with Dunnett's post hoc test.

with various biological networks as an upstream regulatory signal in response to hypercapnia, which could help explain the significant effects of high CO₂ on different cells and organisms^{3,7,9-18}.

Alterations in expression of Wnt pathway genes may be of central importance in the systems-level understanding of organismal effects and pathobiology of hypercapnia. Despite different exposure conditions of hypercapnia in each microarray dataset, we observed multiple gene components of the Wnt pathway including Inositol triphosphate receptor gated Ca²⁺ channel and cAMP response element binding protein (CREB) binding protein across species (Fig. S1). Furthermore, we found the hypercapnia-responsive transcription factors such as c-Myc, Oct-4 and c-Jun which are the target genes of the Wnt signaling across mouse tissues exposed to hypercapnia. *In vitro* experiments with the same levels of exposure suggest transient increases in expressions of Frizzled and Wnt ligand genes in cultured cells from different origins including epithelial, smooth muscle, skeletal muscle and macrophage-like lineage in mice, humans and *Drosophila*. Although the magnitude of hypercapnia and gene expression profile of the Wnt signaling pathway differ between each dataset, the biological interpretation of our data point to significant activation of Wnt pathway genes, suggesting an evolutionary role of elevated CO₂ on Wnt signaling. Wnt signals can activate at least two distinct intracellular signaling, canonical or non-canonical pathways²³. The canonical Wnt/ β -catenin pathway is characterized by cytosolic and nuclear β -catenin accumulation and the activation of certain β -catenin-responsive target genes. The non-canonical β -catenin-independent

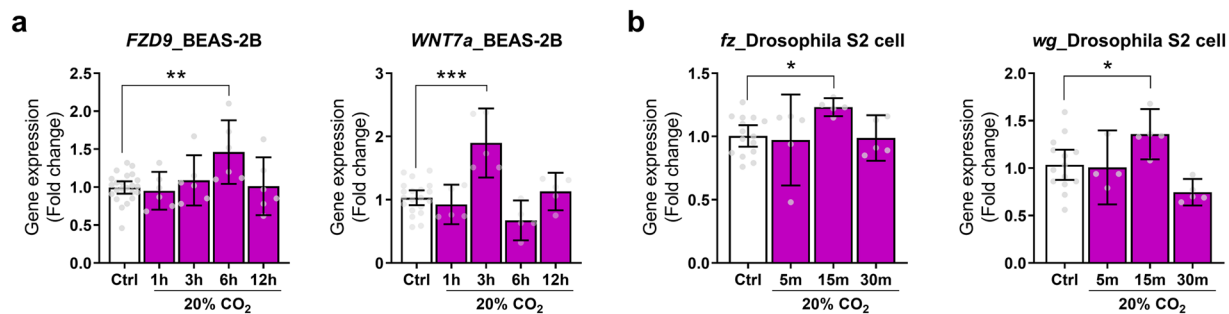


Figure 3. Validation of the transcriptomic datasets of hypercapnia in a human bronchial cell line and invertebrates. **(a)** *FZD9* and *WNT7a* expression in BEAS-2B cells exposed to high CO₂ for up to 12 hours (Ctrl, n = 20–23; 20%CO₂, n = 5–6 per group). Ctrl, control conditions. **(b)** *Fz* and *wg* expression in *Drosophila* S2 cells exposed to high CO₂ for up to 30 min (Ctrl, n = 14–15; 20%CO₂, n = 4–5 per group). All values are represented as mean with error bars shown as the 95% confidence interval. *p < 0.05, **p < 0.01, ***p < 0.001, one-way ANOVA with Dunnett’s post hoc test.

pathways include the calcium/calmodulin-dependent kinase II (CaMKII)-mediated Wnt/Ca²⁺ pathway and the small GTPase RhoA- and Jun N-terminal kinase (JNK)-dependent planar cell polarity pathway. Specifically, Wnt7a rapidly induces the local activation of CaMKII²⁶ and directly interacts with Fzd9 to inhibit cell growth via activation of the JNK pathway²⁷. Overexpression of Wnt7a increases expression of the Wnt-target transcription factor genes including c-Myc^{28,29} and c-Jun²⁸. c-Myc can bind to the *Fzd9* gene promoter and promotes *Fzd9* expression³⁰. Hypercapnia may activate the Wnt7a/Fzd9 signal, setting up a feedback loop via Wnt-target transcription factors that could enhance the Wnt pathway genes. It has also been suggested that Wnt signals activate a metabolic sensor AMP-activated protein kinase (AMPK) in myotubes²⁴ and muscle-specific RING finger protein-1 (MuRF-1) leading to muscle atrophy³¹. Interestingly, we have reported that CaMKII, RhoA, JNK, AMPK and MuRF1 are responsive to hypercapnia in physiological contexts. In mammals, hypercapnia impairs cell proliferation¹⁴ and alveolar fluid reabsorption via a Ca²⁺/JNK pathway^{4,9,17}, leads to airway constriction via Ca²⁺/RhoA axis signaling⁷, AMPK/MuRF-1-dependent muscle atrophy¹¹, and adipogenesis via CREB activation¹³. Hypercapnia is also known to induce Na,K-ATPase endocytosis in *Drosophila melanogaster*¹⁷ and lower fertility in *Caenorhabditis elegans*¹⁷ via activation of the JNK pathway. Together with these reports, our data suggest a linkage of Wnt signaling to the pathobiological changes induced by hypercapnia^{4,7,9,11,17}.

Why elevated CO₂ levels activate Wnt signaling in different tissues/cells and species is not completely understood. Wnt signaling pathway is one of the major pathways regulating tissue architecture during development and in homeostasis of adult tissues³². In the mammalian lung system, Wnt signal maintains stemness of alveolar type 2 cells and can trigger transdifferentiation into alveolar type 1 cells which are part of the gas exchange surface of the lung alveolus³³. We reason that Wnt response during CO₂ elevation (which occurs in human lung diseases) may represent an adaptive homeostatic mechanism against stress to preserve organismal function during noxious alterations in gaseous (CO₂) levels. However, such a mechanism may well become maladaptive to cells, organs and organisms as observed in during prolonged hypercapnia^{7–18}.

In summary, our transcriptomic analysis of multiple datasets revealed a previously unknown role of hypercapnia in the regulation of gene expression. We found a conserved genomic response to hypercapnia regulating Wnt pathway genes in lung and skeletal tissues and cells in mice, bronchial epithelial cells in humans as well as in flies and nematodes.

Methods

Reagents. All cell culture reagents were purchased from Corning Life Sciences. All chemicals were purchased from Sigma-Aldrich. Reagents for quantitative polymerase chain reaction (qPCR) were purchased from Life Technologies. The mRNA Isolation Kit was purchased from QIAGEN.

Animals. Adult (9–11 weeks old) C57BL/6J male mice were obtained from the Jackson Laboratories (Bar Harbor, ME). All animals were provided with food and water *ad libitum*, maintained on a 14-hour light/10-hour dark cycle, and handled according to National Institutes of Health guidelines. All of the procedures involving animals were approved by the Northwestern University Institutional Animal Care and Use Committee (IS0000245 and IS00010662). For high CO₂ exposure, animals were maintained in a Biospherix C-Shuttle Glove Box (BioSpherix) for 3 or 7 days. The chamber’s atmosphere was continuously monitored and adjusted with ProOx/ProCO₂ controllers (BioSpherix) in order to maintain 10% CO₂ and 21% O₂, with a temperature of 20°C–26°C and a relative humidity between 30% and 50%. These settings resulted in arterial partial pressure of carbon dioxide (PaCO₂) of ~80 mmHg and PaO₂ of ~100 mmHg, whereas in animals maintained in room air PaCO₂ was ~40 mmHg and PaO₂ was ~100 mmHg^{10,11}. The values of high PaCO₂ are representative of CO₂ levels encountered in patients with COPD and mechanically ventilated patients with the “permissive hypercapnia” modality^{7,22}. The pH, PaCO₂, and PaO₂ values obtained after exposure to 10% CO₂ for 3 or 7 days were very similar to the values achieved during renal compensation and distinct from acute respiratory acidosis^{10,11}. None of the animals developed appreciable distress. At selected time points, animals were euthanized with Euthasol (pentobarbital

sodium–phenytoin sodium) and trachea, whole lung, diaphragm and soleus were harvested. Then the tissues were snap-frozen in liquid nitrogen for RNA extraction.

Mouse multi-tissue microarray. Total RNA from skeletal muscle tissues was isolated with the miRNeasy Mini kit (Qiagen, Valencia, CA). Messenger RNA profiling was performed with an Agilent SurePrint G3 8 × 15K mouse microarray containing 39,430 messenger RNAs (Sanger miRbase release 9.1), in accordance with the protocol described by the manufacturer (Agilent) and as previously described³⁴. Results were compared by unpaired *t* test, and gene expression was considered to be significantly different between groups when $p < 0.05$. For lung transcriptomic analysis, we used the transcriptomic datasets previously described by us⁷. The lists of DEGs in each dataset were obtained by ≥ 1.4 fold-change with an adjusted *p* value ≤ 0.05 . The identified DEGs were analyzed in the PANTHER classification system (<http://www.pantherdb.org/>) to determine enriched biological processes and categorize into signaling pathways. Gene signatures representing lung, diaphragm or soleus transcriptome changes in hypercapnia were further subjected to functional gene network analysis. Functional Gene Set Enrichment Analysis (FGSEA) was used to generate functional gene networks by metagrouping of individual gene term sets (referencing GO Biological Process and KEGG Pathways), based on function similarity. The GeneTerm Linker algorithm implemented in the “FGNet” package (R) was used to perform the analysis, which utilized nonredundant reciprocal linkage of genes and biological terms³⁵. This methodology filters enrichment output results through reciprocal linkage between genes and terms to produce functional metagroups of key biological significance. Parameters set for this analysis included adjusted *p*-value < 0.05 , minimum gene term support of 3. Genes were deemed “functional hub” genes if they belonged to more than one functional metagroup, suggesting a central role in regulation of biological processes. Networks generated utilizing this analysis were exported in GLM format for further analysis and visualization, using the “iGraph” package (R). Cytoscape 3.2.1 was used for analysis of edge weight, node connectivity, and betweenness within the networks. Transcription factors were not directly measured in our data but inferred from gene expression signatures based on unbiased predictive analysis of known upstream regulators of differentially expressed genes. This analysis was performed in GeneGO Metacore (Thomson Reuters). Venn diagrams were used to determine conserved representation of inferred transcription factors across different tissues and timed responses in hypercapnia.

Secondary analysis of available transcriptomic datasets of hypercapnia. Data from three studies investigating the transcriptomic response to hypercapnia in human bronchial epithelial cells (GSE110362), *Caenorhabditis elegans*¹⁸ and *Drosophila melanogaster* (GSE17444) were obtained. Differential expression analysis of each processed dataset was performed with ≥ 1.4 fold-change with an adjusted *p* value ≤ 0.05 in the PANTHER pathways classification system.

Cells lines and culture. MLE-12 cells (CRL-2110; ATCC) were grown in Dulbecco’s modified Eagle’s medium (DMEM) supplemented with 10% fetal bovine serum (FBS), penicillin (100 U/ml), and streptomycin (100 µg/ml; culture medium).

Mouse ASM cell isolation and culture were performed as described elsewhere⁷. Briefly, the trachea from C57BL/6J mice was removed and transferred into culture medium. Connective tissue and airway epithelium were removed by firmly scraping the luminal surface. The trachea strips were cut into small pieces (~1 mm³) and cultured in culture medium at 37 °C in 5% CO₂. ASM cells begin to migrate out of the fragments after 7 to 10 days. The cells were dissociated with 0.05% trypsin and subcultured in culture medium. Identification of mouse ASM cells was based on the morphology and expression of α-SMA. Mouse ASM cells of passage <6 were used in all the experiments.

C2C12 mouse myoblasts (ATCC, CRL1772) were cultured and differentiated as described elsewhere¹¹. In brief, cells were allowed to grow in plates until they reached ~90–95% confluence, and then culture media was changed to DMEM supplemented with 2% horse serum (differentiation media) for C2C12 myotube experiments. The differentiation media was renewed every 18–24 h, and cells were allowed to differentiate for 3 days.

Immortalized human bronchial epithelial cell line BEAS-2B were obtained from ATCC (CRL-9609) and grown in culture medium.

Drosophila S2 cells were obtained from the Dr. Silverman’s laboratory (University of Massachusetts Medical School).

CO₂ medium and CO₂ exposure for mammalian cells. For the different experimental conditions, initial solutions were prepared with DMEM/Ham’s F-12 medium/Tris base/MOPS base (3:1:0.25:0.25) containing 10% FBS or 2% horse serum, 100 U/mL penicillin, and 100 µg/mL streptomycin, as described elsewhere^{7,11}. The buffering capacity of the medium was modified by changing its initial pH with Tris and MOPS base to obtain a pH of 7.4 at the various CO₂ levels (pCO₂ of 40 or ~120 mm Hg). In our prior work, the maximal effects of hypercapnia on signal transduction pathways was achieved at ~120 mmHg of CO₂ with short (minute to hour) exposure conditions in lung cells^{7,9,17} and skeletal muscle cells¹¹, the subsequent cellular experiments with high CO₂ were performed under these conditions. Lower CO₂ levels also activate the signaling pathways and have pathophysiological effects but with more prolonged exposures. The desired CO₂ and pH levels were achieved by equilibrating the medium overnight in a humidified chamber (C-Chamber, BioSpherix, Lacona, NY). The atmosphere of the C-Chamber was controlled with a PRO CO₂ carbon dioxide controller (BioSpherix). In this chamber, cells were exposed to the desired pCO₂ while maintaining 21% O₂ balanced with N₂. Before CO₂ exposure, pH, pCO₂, and pO₂ levels in the medium were measured using a Stat Profile pHox blood gas analyzer (Nova Biomedical, Waltham, MA). Experiments began by replacing the culture medium with the CO₂-equilibrated medium and incubating in the C-Chamber for the desired time.

Maintenance of *Drosophila* S2 cells and CO₂ exposure. *Drosophila* S2 cells were grown at room temperature and protected from light in Schneider's insect medium containing 10% FBS (Valley Biomedical) and 0.2% Penicillin-Streptomycin (GIBCO). For cell attachment, plates were treated with 1 N HCl for 1 hour, washed 3 times with sterile water, 0.5 mg/mL Concanavalin A (Sigma) for 1 hour, washed once with sterile water. S2 cells were plated at a density of 2.0×10^6 cell per well in six-well plates with the medium and allowed to attach for 1 hour. For high CO₂ treatments, initial solutions were prepared with Schneider's insect medium/Tris base/MOPS base (4:0.25:0.25) containing 10% FBS, 100 U/mL penicillin, and 100 µg/mL streptomycin. The buffering capacity of the medium was modified by changing its initial pH with Tris and MOPS base to obtain a pH of 7.2 at the CO₂ level of ~120 mm Hg. The desired CO₂ and pH levels were achieved by equilibrating the medium overnight in a C-Chamber protected from light and at room temperature. The atmosphere of the C-Chamber was controlled with a PRO CO₂ carbon dioxide controller. Before CO₂ exposure, pH, pCO₂, and pO₂ levels in the medium were measured using a Stat Profile pHox blood gas analyzer. Experiments were started by replacing the culture medium with the CO₂-equilibrated medium and incubating at room temperature and protected from light for the desired time.

Quantitative reverse transcription PCR. To isolate total RNA from tissues and cells were homogenized directly in 700 µL of lysis/binding buffer provided by the miRNeasy Mini kit (Qiagen). Complementary DNA was synthesized from 1 µg of total RNA using a qScript cDNA Synthesis kit (Quanta Biosciences, Beverly, MA) and mRNA expression level was determined by quantitative PCR (qPCR) using SYBR Green chemistry (Bio-Rad). Relative expression of the transcripts was determined according to the $\Delta\Delta C_t$ method using *Rpl19* for mouse, *RPL19* for BEAS-2B or *Rpl32* for *Drosophila* S2 cells as reference for normalization.

Statistical analysis. Statistical methods are described in the figure legends and in the relevant methods descriptions. Sample size (n) values used for statistical analyses are provided in the relevant figures. Exclusion criteria were pre-established. Individual samples may have been excluded on the basis of sample processing error during experimental work-flow. Statistical outliers were detected and removed based on Grubbs' test criteria when appropriate. For qRT-PCR data analysis, normally distributed data were analyzed by parametric tests including an unpaired two-tailed Student's t test for two-group comparisons or a one-way ANOVA for multiple comparisons with Dunnett's post-hoc corrections for three or more groups. Variances were examined by F test or the Brown-Forsythe test. Statistical analysis was performed using GraphPad Prism (version 7.02, GraphPad Software). p values of < 0.05 were considered to be significant. All values are represented as means with error bars shown as the 95% confidence interval.

Data availability

The microarray data of mouse skeletal muscle tissues generated in this project can be found in Supplement (Data S1).

Received: 26 May 2019; Accepted: 14 November 2019;

Published online: 03 December 2019

References

- Weir, E. K., Lopez-Barneo, J., Buckler, K. J. & Archer, S. L. Acute oxygen-sensing mechanisms. *N. Engl. J. Med.* **353**, 2042–2055 (2005).
- Haldar, S. M. & Stamler, J. S. S-nitrosylation: integrator of cardiovascular performance and oxygen delivery. *J. Clin. Invest.* **123**, 101–110 (2013).
- Cummins, E. P., Selfridge, A. C., Sporn, P. H., Sznajder, J. I. & Taylor, C. T. Carbon dioxide-sensing in organisms and its implications for human disease. *Cell. Mol. Life Sci.* **71**, 831–845 (2014).
- Shigemura, M., Lecuona, E. & Sznajder, J. I. Effects of hypercapnia on the lung. *J. Physiol.* **595**, 2431–2437 (2017).
- Laffey, J. G. & Kavanagh, B. P. Carbon dioxide and the critically ill—too little of a good thing? *Lancet* **354**, 1283–1286 (1999).
- listed, Na Ventilation with lower tidal volumes as compared with traditional tidal volumes for acute lung injury and the acute respiratory distress syndrome. The Acute Respiratory Distress Syndrome Network. *N. Engl. J. Med.* **342**, 1301–1308 (2000).
- Shigemura, M. *et al.* Hypercapnia increases airway smooth muscle contractility via caspase-7-mediated miR-133a-RhoA signaling. *Sci. Transl. Med.* **10** (2018).
- Bharat, A. *et al.* Pleural Hypercarbia After Lung Surgery Is Associated With Persistent Alveolepleural Fistulae. *Chest* **149**, 220–227 (2016).
- Vadasz, I. *et al.* AMP-activated protein kinase regulates CO₂-induced alveolar epithelial dysfunction in rats and human cells by promoting Na,K-ATPase endocytosis. *J. Clin. Invest.* **118**, 752–762 (2008).
- Gates, K. L. *et al.* Hypercapnia impairs lung neutrophil function and increases mortality in murine pseudomonas pneumonia. *Am. J. Respir. Cell Mol. Biol.* **49**, 821–828 (2013).
- Jaitovich, A. *et al.* High CO₂ levels cause skeletal muscle atrophy via AMP-activated kinase (AMPK), FoxO3a protein, and muscle-specific Ring finger protein 1 (MuRF1). *J. Biol. Chem.* **290**, 9183–9194 (2015).
- Casalino-Matsuda, S. M. *et al.* Hypercapnia Alters Expression of Immune Response, Nucleosome Assembly and Lipid Metabolism Genes in Differentiated Human Bronchial Epithelial Cells. *Sci. Rep.* **8**, 13508 (2018).
- Kikuchi, R. *et al.* Hypercapnia Accelerates Adipogenesis: A Novel Role of High CO₂ in Exacerbating Obesity. *Am. J. Respir. Cell Mol. Biol.* **57**, 570–580 (2017).
- Vohwinkel, C. U. *et al.* Elevated CO₂ levels cause mitochondrial dysfunction and impair cell proliferation. *J. Biol. Chem.* **286**, 37067–37076 (2011).
- Nilsson, G. E. *et al.* Near-future carbon dioxide levels alter fish behaviour by interfering with neurotransmitter function. *Nature Climate Change* **2**, 201–204 (2012).
- Helenius, I. T. *et al.* Elevated CO₂ suppresses specific *Drosophila* innate immune responses and resistance to bacterial infection. *Proc. Natl. Acad. Sci. USA* **106**, 18710–18715 (2009).
- Vadasz, I. *et al.* Evolutionary conserved role of c-Jun-N-terminal kinase in CO₂-induced epithelial dysfunction. *PLoS One* **7**, e46696 (2012).
- Sharabi, K. *et al.* Elevated CO₂ levels affect development, motility, and fertility and extend life span in *Caenorhabditis elegans*. *Proc. Natl. Acad. Sci. USA* **106**, 4024–4029 (2009).
- Taylor, C. T. & Cummins, E. P. Regulation of gene expression by carbon dioxide. *J. Physiol.* **589**, 797–803 (2011).

20. Barreiro, E., Sznajder, J. I., Nader, G. A. & Budinger, G. R. Muscle dysfunction in patients with lung diseases: a growing epidemic. *Am. J. Respir. Crit. Care Med.* **191**, 616–619 (2015).
21. Zhang, J. *et al.* Insights into the Molecular Mechanisms of CO₂-Mediated Regulation of Stomatal Movements. *Curr. Biol.* **28**, R1356–R1363 (2018).
22. Nin, N. *et al.* Severe hypercapnia and outcome of mechanically ventilated patients with moderate or severe acute respiratory distress syndrome. *Intensive Care Med.* **43**, 200–208 (2017).
23. Sethi, J. K. & Vidal-Puig, A. Wnt signalling and the control of cellular metabolism. *Biochem. J.* **427**, 1–17 (2010).
24. Abiola, M. *et al.* Activation of Wnt/beta-catenin signaling increases insulin sensitivity through a reciprocal regulation of Wnt10b and SREBP-1c in skeletal muscle cells. *PLoS One* **4**, e8509 (2009).
25. Tsai, H. L. *et al.* Wnts enhance neurotrophin-induced neuronal differentiation in adult bone-marrow-derived mesenchymal stem cells via canonical and noncanonical signaling pathways. *PLoS One* **9**, e104937 (2014).
26. Ciani, L. *et al.* Wnt7a signaling promotes dendritic spine growth and synaptic strength through Ca(2+)-/Calmodulin-dependent protein kinase II. *Proc. Natl. Acad. Sci. USA* **108**, 10732–10737 (2011).
27. Winn, R. A. *et al.* Restoration of Wnt-7a expression reverses non-small cell lung cancer cellular transformation through frizzled-9-mediated growth inhibition and promotion of cell differentiation. *J. Biol. Chem.* **280**, 19625–19634 (2005).
28. Zhao, L. *et al.* An integrated analysis identifies STAT4 as a key regulator of ovarian cancer metastasis. *Oncogene* **36**, 3384–3396 (2017).
29. Dong, L. *et al.* A Conditioned Medium of Umbilical Cord Mesenchymal Stem Cells Overexpressing Wnt7a Promotes Wound Repair and Regeneration of Hair Follicles in Mice. *Stem Cells Int.* **2017**, 3738071 (2017).
30. Lawlor, E. R. *et al.* Reversible kinetic analysis of Myc targets *in vivo* provides novel insights into Myc-mediated tumorigenesis. *Cancer Res.* **66**, 4591–4601 (2006).
31. Rajasekaran, M. R. *et al.* Age-related external anal sphincter muscle dysfunction and fibrosis: possible role of Wnt/beta-catenin signaling pathways. *Am. J. Physiol. Gastrointest. Liver Physiol.* **313**, G581–G588 (2017).
32. Clevers, H. Wnt/beta-catenin signaling in development and disease. *Cell* **127**, 469–480 (2006).
33. Nabhan, A. N., Brownfield, D. G., Harbury, P. B., Krasnow, M. A. & Desai, T. J. Single-cell Wnt signaling niches maintain stemness of alveolar type 2 cells. *Science* **359**, 1118–1123 (2018).
34. Konishi, K. *et al.* Gene expression profiles of acute exacerbations of idiopathic pulmonary fibrosis. *Am. J. Respir. Crit. Care Med.* **180**, 167–175 (2009).
35. Fontanillo, C., Nogales-Cadenas, R., Pascual-Montano, A. & De las Rivas, J. Functional analysis beyond enrichment: non-redundant reciprocal linkage of genes and biological terms. *PLoS One* **6**, e24289 (2011).

Acknowledgements

We would like to thank Diego A. Celli (Division of Pulmonary and Critical Care, Department of Medicine, Feinberg School of Medicine, Northwestern University) and K.V. Pandit (Division of Pulmonary, Allergy and Critical Care Medicine, University of Pittsburgh School of Medicine) for their technical assistance. This work was supported in part by the US National Institutes of Health (HL-071643, HL-147070, HL-107629 and HL-131745). M.S. was a David W. Cugell fellow. E.P.C. is funded by Science Foundation Ireland (15/CDA/3490).

Author contributions

M.S., E.L. and J.I.S. contributed to all study design and data interpretation and wrote the manuscript. M.A. and N.K. performed microarray experiments, and M.S., M.A., M.B.E. and S.B. analyzed the data. M.S. and L.C.W. executed animal experiments and analyzed the data. L.A.D., L.C.W., S.M.C.M., P.H.S.S., I.V., I.T.H., G.A.N., Y.G., K. S., E.P.C., C. T., A.B., C.J.G., G.J.B., G.R.S.B. and S.B. interpreted the data and wrote the paper. J.I.S., P.H.S.S. and G.R.S.B. provided funding and resources.

Competing interests

The authors declare no competing interests.

Additional information

Supplementary information is available for this paper at <https://doi.org/10.1038/s41598-019-54683-0>.

Correspondence and requests for materials should be addressed to J.I.S.

Reprints and permissions information is available at www.nature.com/reprints.

Publisher's note Springer Nature remains neutral with regard to jurisdictional claims in published maps and institutional affiliations.



Open Access This article is licensed under a Creative Commons Attribution 4.0 International License, which permits use, sharing, adaptation, distribution and reproduction in any medium or format, as long as you give appropriate credit to the original author(s) and the source, provide a link to the Creative Commons license, and indicate if changes were made. The images or other third party material in this article are included in the article's Creative Commons license, unless indicated otherwise in a credit line to the material. If material is not included in the article's Creative Commons license and your intended use is not permitted by statutory regulation or exceeds the permitted use, you will need to obtain permission directly from the copyright holder. To view a copy of this license, visit <http://creativecommons.org/licenses/by/4.0/>.

© The Author(s) 2019